Influence of Oxygen on the UV−Photocatalyzed Generation of Pyrene Cation Radicals in the Zeolites X and Y

Eric H. Ellison*

Department of Chemistry and Biochemistry, 322 Coulter Hall, University of Mississippi, University, Mississippi 38677

Received: June 12, 2003; In Final Form: February 11, 2004

The photoinduced generation of pyrene cation radicals ($Py^{+}\cdot$) has been examined as a function of oxygen pressure in the internal cavities of the zeolites NaX and NaY. Excitation of pyrene was carried out at ultraviolet wavelengths by utilizing either a pulsed laser or a steady-state arc lamp. For lamp-irradiated samples, the generation of long-lived $Py^{+}\cdot$ was monitored during the course of irradiation by visible-wavelength absorption spectroscopy. In dehydrated NaX (dNaX), irradiation of pyrene in the presence of 0.01−1 bar O_2 produced an approximately 10-fold increase in the yield of $Py^{+}\cdot$ relative to samples irradiated under evacuated conditions. By contrast, when pyrene was irradiated in dehydrated NaY (dNaY), no increase in $Py^{+}\cdot$ yield was observed at any O_2 pressure relative to evacuated conditions. However, in hydrated NaY, O_2-induced increases in $Py^{+}\cdot$ yield were observed, while no similar increases were observed in hydrated NaX. Following laser excitation of samples, the yield, stability, and reactivity of $Py^{+}\cdot$ were monitored by transient absorption spectroscopy. The transient studies revealed differences in the yield of $Py^{+}\cdot$ that were in accord with the lamp studies, but only when the effects of O_2 on two-photon ionization were properly accounted for. An efficient back-reaction of $Py^{+}\cdot$ with superoxide ($O_2^{-}\cdot$) is postulated in hydrated NaX, to account for the absence of $Py^{+}\cdot$ in the lamp studies. A direct excited-state electron-transfer mechanism (type I) is favored for the O_2-induced generation of $Py^{+}\cdot$ in zeolites, and it is supported by results which rule out mechanisms involving singlet oxygen and the reaction of O_2 with trapped electrons that would otherwise recombine with $Py^{+}\cdot$. Comparisons of the fluorescence spectrum and lifetime of pyrene in dNaX and dNaY show that pyrene encounters a microenviroment of unusually high polarity in dNaY. It is suggested that the highly polar interaction is related to the electrophilicity of dNaY and is characteristic of a type of charge-transfer interaction that draws electron density from pyrene and prevents the excited state from donating an electron to O_2. Such an interaction does not occur in dNaX, which is known to be less electrophilic or more electronegative than dNaY. In hydrated NaY, the presence of water weakens the strongly polar interaction and allows the electron transfer to occur. This study illustrates an important difference between zeolites that vary in electronegativity and how photoinduced charge separation involving neutral molecules is affected by hydration of the zeolite.

Introduction

Zeolites are crystalline, microporous aluminosilicates that can be synthesized in the laboratory or, in some cases, found naturally as mineral deposits. One important industrial application of zeolites is in petroleum refining, where they are used as catalysts and molecular sieves under extreme conditions. Zeolites are also commonly used as sorbents and as ion-exchange media in a variety of industrial processes.[1−4] Other applications of zeolites continue to be pursued, given the many unique and interesting features of molecular and ionic behavior that have been observed in zeolites.

Since the early 1980s, photochemists have explored the use of zeolites as a reaction medium and literature reviews are available on the subject.[5−9] These studies have shown how zeolites can be strategically used to gain a photophysical or photochemical advantage, and have provided a detailed description of molecular behavior that has assisted the development of new and existing applications of zeolites in general. Current research on photochemistry in zeolites that continues to draw upon the earlier findings includes such topics as wireless solar energy conversion or photocatalysis[10−14] and fine chemical synthesis that relies on selective oxidation[15−17] and chiral induction.[18]

While studies of photochemistry in solution are assisted by knowledge of solvent properties, studies of photochemistry in zeolites are assisted by the vast amount of chemical and structural information that is already known about zeolites.[1,2] Zeolites with properties that can be varied through straightforward synthetic or postsynthetic treatments are particularly advantageous, because they allow for a more complete survey of medium effects and potential for control of molecular behavior. The majority of photochemical studies on zeolites have utilized the zeolites X and Y, which are synthetic analogues of the naturally-occurring mineral faujasite. The pore opening of these materials ranges from 7 to 8 Å in diameter[19] and is the largest of the inexpensive, commercially available zeolites. The internal cavities consist of α-cages (or supercages) which are 13 Å in diameter, and β-cages (or sodalite cages) which are 6.6 Å in diameter. The pore opening to the β-cage is only 2.2 Å and too small to be penetrated by any molecule other than water. Given their relatively large pore and cavity size, a much

* Corresponding author. E-mail: eellison@olemiss.edu.

10.1021/jp0356766 CCC: $27.50
Published on Web 03/24/2004

wider range of photosystems can be included in the internal cavities of the zeolites X and Y compared to most other zeolites.

As a photochemical medium, one rationale for using zeolites is to promote photoinduced charge separation between two molecules. In some cases, the zeolite cage or pore architecture is used to exert control over the relative spatial locations of the donor and acceptor molecules undergoing electron transfer. This is the case, for example, in studies of electron-transfer involving trisbipyridyl ruthenium(II) and bipyridinium salts in zeolites.[11,13,14] In other cases, the zeolite is used simply as a polar or "superpolar"[20] medium to modulate back electron transfer following photoexcitation of charge-transfer complexes[21] and sensitizer-acceptor systems.[10,22,23] Typically, zeolites are negatively charged by virtue of the substitution of aluminum for silicon in their framework structure. These zeolites contain exchangeable cations, many of which are located on the walls of the internal cavities. In the absence of polar solvents, molecules in association with the wall cations encounter large electrostatic fields, or a high degree of surface polarity. The interaction of molecules with the exposed cations is unique and sometimes creates unusual behavior that can be taken advantage of.

One current issue is the nature of photoinduced electron transfer from included molecules to molecular oxygen (O_2) in zeolites. A notable effect discovered by Frei and co-workers in the early 1990s was the selective, photocatalyzed oxidation of small hydrocarbon molecules by visible excitation of hydrocarbon$-O_2$ CT complexes in zeolites.[15,24] While this topic has since been pursued in more detail by Frei's group and others,[16,25,26] there has been little emphasis on the reaction of excited singlet or triplet states of similar species with O_2 in zeolites. Much of the previous work in zeolites has focused on either luminescence quenching by O_2 or product formation and has not pursued any details concerning the mechanism of electron transfer.

In the present study, photoinduced electron transfer between pyrene and O_2 is explored in the sodium ion-exchanged forms of zeolites X and Y. The low gas-phase ionization potential of pyrene (i.e., 7.4 eV) makes it suitable as an electron donor for this study. Some initial discoveries were made when zeolite samples containing pyrene were irradiated at ultraviolet wavelengths with a steady-state arc lamp in either the presence or absence of oxygen. In dehydrated NaX, a dramatic increase in the yield of pyrene cation radicals ($Py^{+\cdot}$) was observed as a result of adding oxygen to the sample. No similar increase was observed in dehydrated NaY. Additional experiments involving laser flash photolysis and fluorescence spectroscopy were designed to explain the mechanism involved, the differences between NaX and NaY, and the effects of hydration of the sample.

Experimental Section

Materials. Powdered forms of the zeolites NaX and NaY were obtained from Aldrich or UOP and have the chemical composition $Na_{80}Al_{80}Si_{112}O_{384}$ (Si/Al = 1.4) and $Na_{55}Al_{55}Si_{137}O_{384}$ (Si/Al = 2.5), respectively. Both zeolites were stirred in excess 1 M NaCl (aq) and thoroughly rinsed with ultrapure Millipore water. Silica gel (Davisil-60) and silica−alumina (both from Aldrich) were used as received. Potassium-exchanged zeolite X was prepared by stirring NaX in excess 1 M KNO_3 (aq) at 70 °C, followed by rinsing. Pyrene was purified by column chromatography using hexane as the mobile phase and activated silica gel as the stationary phase. The product of the separation was a pure white solid. Methylene blue was obtained from Sigma and used as received.

Sample Preparation. Zeolite powders were pressed into thin (100 μm-thick) pellets and dried in air at 550 °C for at least 15 min. After the pellets were cooled under a flowing stream of dry N_2, they were transferred to solutions of pyrene in cyclohexane and agitated for at least 2 h on an orbital shaker. From a quantitative analysis of the supernatant, pyrene was found to be >97% adsorbed from cyclohexane solutions when the desired loading was 0.002/supercage. Loaded samples were transferred to 10-mm × 1-mm evacuable suprasil cells and evacuated to milliTorr pressures at 125 °C for 15 min in order to remove the cyclohexane and small amounts of H_2O. A previous study has shown the effectiveness of this thermal treatment for removing water from samples.[27] Essentially, water is removed to a level equivalent to heating the zeolite for several hours at 550 °C in air. All spectroscopic measurements were made at pyrene loadings between 0.001 and 0.002 per supercage, and on samples housed in evacuated quartz cells that were sealed with ultrahigh-vacuum stopcocks. Each sample contained a total of 5−10 nmol of Py.

Oxygen was added to evacuated samples through the vacuum line from an O_2 reservoir. The O_2 pressure was measured to the nearest mbar by using a digital vacuum gauge. The total cell volume was ca. 5 mL, meaning that at 1 mbar O_2 and 298 K, there was 200 nmol O_2 in the cell. Thus, even at low P_{O_2}, the amount of O_2 is much higher than that of Py, ensuring that pseudo first-order conditions regarding quenching by O_2 are obeyed.

Water was added in controlled fashion to evacuated and dehydrated samples through the vacuum line from the vapor phase. Following the addition of water, the sample was heated for 15 min at 80 °C with the vacuum tap closed to ensure a uniform distribution of water in the sample. The water content of the sample was determined by gravimetric analysis to the nearest 0.01 mg, in accord with a previous approach.[27]

Instrumentation. Fluorescence was measured by steady-state and time-resolved approaches, employing 45° front-face excitation and collection. The steady-state instrument was a Jobin-Yvon Fluoromax-3 spectrofluorometer. Time-resolved measurements were made by excitation with 0.5-ns pulses from a PTI GL-3300 nitrogen laser (λ = 337.1 nm). The emission was passed through an Oriel 77200 monochromator and detected with a photosensor having a rise time of 0.78 ns. A Tektronix TDS-3052B digitizing oscilloscope (500 MHz bandwidth) was used to capture and store the decay profiles for computer analysis. Fitting of the decay profiles to a Gaussian distribution in the natural logarithm of decay rates was carried out as previously described.[8, 28]

Transient absorption spectra were measured in the diffuse transmittance mode following excitation with single pulses from the fourth harmonic of a Continuum Surelite-I Nd:YAG laser (λ_{ex} = 266 nm, τ_{pulse} = 5 ns, E_{pulse} = 5 mJ) or the nitrogen laser. The detector was a CCD array spectrometer coupled to fiber optic cables and triggered by the laser pulse. The analyzing light source was a 2-μs pulse from a xenon flashlamp. Delay of the pulsed analyzing light following excitation was controlled from 12 μs outward by using a digital pulse generator.

Decay profiles of absorbance were measured in the diffuse transmittance mode following pulsed laser excitation. The analyzing light source was either the steady-state or ms-pulsed output of a 450 W xenon arc lamp (Edinburgh Analytical Instruments Xe900 and Xp900). An Oriel Model 77200 monochromater was used to select the analyzing wavelength, and a Hamamatsu R955 photomultiplier tube was used as the detector.

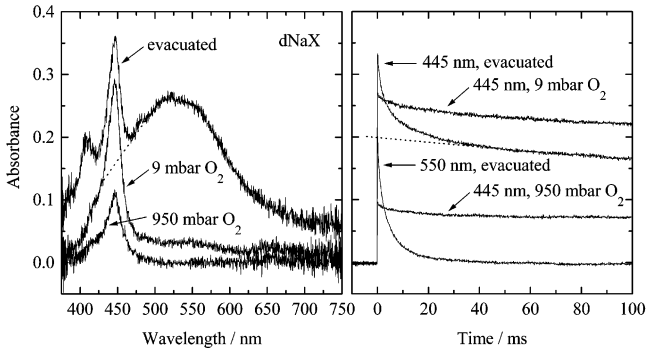

Figure 1. The effect of P_{O_2} on the absorption spectrum and decay profile following 266-nm, 5-ns pulsed laser excitation of pyrene in dehydrated NaX. The left graph illustrates the spectra taken at 12 μs following excitation with a single laser pulse. The right graph illustrates the decay profiles of absorbance measured over the course of 100 ms and following a single laser pulse. The pyrene loading was 0.002/supercage.

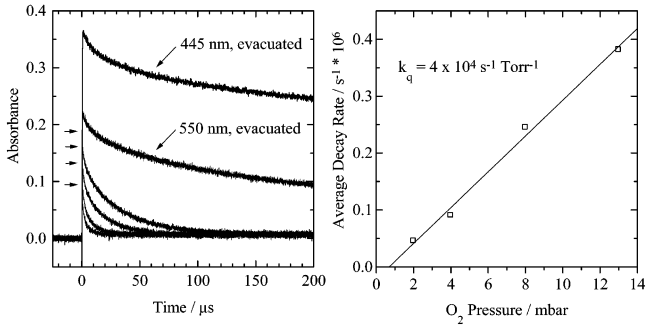

Figure 2. Microsecond decay profiles of absorbance and the plot of average decay rate versus P_{O_2} in dNaX. Left graph at 10 μs from top to bottom: evacuated (445 nm); evacuated (550 nm); P_{O_2} = 2, 4, 8, and 13 mbar (550 nm). The arrows point to the initial intensity of the decays in the presence of O_2 (not observable in the graph) and indicate a decrease in initial intensity with increasing P_{O_2}. The spacing between points in the decay profiles was 40 ns.

Results

Oxygen-Enhanced Formation of Pyrene Cation Radicals. Figure 1 (left graph) illustrates the visible absorption spectrum at 12 μs following 5-ns pulsed excitation of pyrene in a sample of dehydrated NaX (dNaX). Peak assignments can be made on the basis of similar studies by Thomas and co-workers[29] and published spectra of triplets[30] and radical ions[31] in solution. In the evacuated system, the spectral bands peaking at 445 and 410 nm originate from the pyrene cation radical ($Py^{+}\cdot$) and triplet ($T_1 = {}^3Py$), respectively. The broadened band peaking at 535 nm originates from the four-ion cluster trapped electron (Na_4^{3+}), which at room temperature is the most stable of all the ion cluster trapped electron species that have been observed in NaX and NaY.[32] The minor peaks at 490 and 520 nm originate from the anion radical ($Py^{-}\cdot$) and ^3Py bands, respectively. The addition of O_2 to the sample leads to quenching of Na_4^{3+}, ^3Py, and $Py^{-}\cdot$, and at P_{O_2} = 950 mbar only $Py^{+}\cdot$ is observed in the spectrum.

The right graph in Figure 1 illustrates the decay profiles over the course of milliseconds of the absorbance at 445 and 550 nm. A comparison is made of evacuated and oxygenated systems. The spectra in Figure 1 illustrate the origin of the decays. In the oxygenated systems, the decay at 445 nm is representative entirely of $Py^{+}\cdot$. In the evacuated system, the decay at 550 nm is representative primarily of Na_4^{3+}, while that at 445 nm it is representative of $Py^{+}\cdot$, ^3Py, and Na_4^{3+}. In both the evacuated and oxygenated systems, $Py^{+}\cdot$ is much longer-lived than Na_4^{3+}. The decay of Na_4^{3+} in the evacuated system may be due to reaction with residual O_2 present at microbar pressures in the vacuum line, but this effect was not pursued in detail.

In the evacuated system, the decay profile at 445 nm consists of a component that decays within 40 ms and a more slowly decaying component. Below it is argued that the more rapid component does not include contributions from the decay of $Py^{+}\cdot$. By assuming this argument is valid, it can be stated that the yield of long-lived $Py^{+}\cdot$ (e.g., that at 80 ms) is higher at P_{O_2} = 9 mbar relative to the evacuated system. A similar effect was observed upon excitation at 337 nm, by using a nitrogen laser (τ_{pulse} = 0.5 ns). At P_{O_2} = 950 mbar, the $Py^{+}\cdot$ yield was much smaller relative to the evacuated system, pointing out that ionization involves sequential, two-photon absorption by the singlet, as reported earlier.[29] An analysis of the rate of quenching of excited pyrene singlets ($S_1 = {}^1Py$) by O_2 shows that the two-photon process is not significantly quenched by O_2 at P_{O_2} = 9 mbar. The rate constant for quenching of ^1Py by O_2 in dNaX and dNaY was evaluated previously by fluorescence spectroscopy and reported to be 1.2×10^7 s^{-1} $Torr^{-1}$.[33] A similar value was determined for the present systems and is reported below in the section on pyrene fluorescence. Using this value, the rate of quenching of ^1Py at P_{O_2} = 950 mbar is 9.1×10^9 s^{-1}, which is competitive with the rate of photon delivery from the laser (i.e., $1/\tau_{pulse} \approx 1/5$ $ns^{-1} = 2 \times 10^8$ s^{-1}). However, at P_{O_2} = 9 mbar the two-photon process remains operative because the rate of quenching is only 8×10^7 s^{-1}, corresponding to an S_1 lifetime of 13 ns. The absorbance decay profiles were also evaluated on a microsecond time scale, with the intent being to explore the possible involvement of $Py^{+}\cdot - Na_4^{3+}$ recombination in increasing the yield of $Py^{+}\cdot$ at low P_{O_2}.

Figure 2 illustrates the microsecond decay profiles at 445 and 550 nm in evacuated and oxygenated dNaX. In the evacuated system, there is no evidence of a decay process that could possibly originate from the recombination of $Py^{+}\cdot$ with Na_4^{3+}. Although at both wavelengths there is a more rapid component that decays within 50 μs, the percentage of the total amplitude of this component is much smaller at 445 nm than at 550 nm and must therefore originate only from the decay of overlapping Na_4^{3+}. If the component was due to $Py^{+} - Na_4^{3+}$ recombination, it would lead to a larger percentage drop in OD at 445 nm relative to 550 nm. This argument relies on the reasonable assumption that for every $Py^{+}\cdot$ observed in the evacuated system, there is an observable Na_4^{3+}, or that photoejected electrons do not react on a sub-microsecond time scale before they are trapped. The question then remains as to whether millisecond recombination is a significant process. When viewing the spectrum in Figure 1, it can be estimated from the peak shape of Na_4^{3+} (see extended dotted line) that Na_4^{3+} accounts for 43% of the optical density at 445 nm in the evacuated system. The decay profiles indicate that Na_4^{3+} accounts for 42% of the optical density at 445 nm, if the decay inside 40 ms is assumed to be due entirely to Na_4^{3+}. This value was determined by extrapolating back to $t = 0$ the decay of $Py^{+}\cdot$ in the region 60−100 ms (as shown in Figure 1), and using the extrapolated value at $t = 0$ as the OD contribution from $Py^{+}\cdot$. The close agreement between the two analyses indicates that the decay at 445 nm inside 40 ms is representative of the decay of Na_4^{3+} and that millisecond recombination is not a significant process. It also indicates that the triplet and anion radical bands contribute weakly to the absorbance at 445 nm, although this is not the case for hydrated systems as shown below.

Figure 2 (left plot) also illustrates the effect of O_2 on the microsecond decay profiles of Na_4^{3+} in dNaX. The horizontal arrows point to the level of the initial absorbance and indicate that a form of static quenching occurs. The right graph illustrates a Stern−Volmer plot of the decay rate estimated from the 1/e decay time of normalized decay profiles versus P_{O_2}. The 1/e (or average) decay time was plotted because fits of the decays to simple exponential functions were not acceptable. The slope of the line yields a value of 4×10^4 s^{-1} $Torr^{-1}$, in close agreement with the previously reported value of 3×10^4 s^{-1} $Torr^{-1}$ determined by pulsed radiolysis.[32a]

Some comments are necessary at this stage regarding the origin of the static quenching in Figure 2. At low P_{O_2}, quenching of the two-photon, electron-generating process is not significant and can therefore be ruled out as the cause. This leaves the following three possibilities: (1) reaction of two-photon-ejected electrons with O_2 prior to their becoming trapped by Na_4^{4+}; (2) rapid reaction of Na_4^{3+} with O_2; and (3) quenching of excited states that would otherwise react with the zeolite to give Na_4^{3+}. Process 3 is unlikely because single-photon electron injection (or electron transfer from the excited state to the zeolite) is likely to occur at a sub-nanosecond rate which is much faster than the rate of quenching of ^1Py by O_2. Process 1 could occur if the photoejected electrons were initially trapped by unstable ion clusters or other sites. These trapped (or quasi-free) electrons may be more accessible than Na_4^{3+} and quenched on a nanosecond time scale. Process 2 is unlikely and will be discussed in more detail below.

Experiments similar to those in Figures 1 and 2 were carried out in dehydrated NaY (dNaY). For brevity these results are not shown graphically here, but are described as follows. In evacuated dNaY, the yields of $Py^{+}\cdot$ and Na_4^{3+} were similar to those observed in dNaX when similar powers of laser excitation were used. However, unlike the result in dNaX, no increase in the yield of long-lived $Py^{+}\cdot$ was observed at low P_{O_2} in dNaY. For example, the $Py^{+}\cdot$ yield at 80 ms was at $P_{O_2} = 10$ mbar the same as that in the evacuated system when the sample was excited at either 266 or 337 nm. Of further importance was that the static process observed in the decay profiles of Na_4^{3+} in dNaX (see Figure 2) was also observed in dNaY, as well as similar rates of quenching of Na_4^{3+} by O_2.

In dNaX, the increased $Py^{+}\cdot$ yield could originate from an excited-state reaction, whereby O_2 reacts with either S_1 or T_1 to give $Py^{+}\cdot$ and superoxide. It could also originate from a reaction with O_2 of trapped electrons that would otherwise recombine with $Py^{+}\cdot$. These electrons could be generated by a one- or two-photon process. It was shown above that microsecond or longer recombination is not a signficant process. Thus, any $Py^{+}\cdot$− Na_4^{3+} recombination must occur by a nanosecond or faster process. The static process observed in Figure 2 raises the possibility that rapid (nanosecond or faster) quenching of Na_4^{3+} trapped electrons occurs. Such quenching could intercept recombination, thereby increasing the yield of $Py^{+}\cdot$. If the static process reflects such a mechanism, then the mechanism should be operative in both NaX and NaY. That the static process was observed in dNaY without increased yields of $Py^{+}\cdot$ reflects that no correlation exists between the static process and increased yields of $Py^{+}\cdot$. Furthermore, the fluorescence quenching studies indicate that O_2 is very mobile in these systems and that the rate of O_2 transport is not the rate-limiting step in the dynamic quenching of Na_4^{3+}. In other words, the reaction of Na_4^{3+} with O_2 is activation controlled. This is due to the fact that Na_4^{3+} is located in the sodalite cage which is inaccessible to O_2.[32a,32d] For this case, direct contact is not possible and the electron transfer must occur by a long-range tunneling mechanism. The static process is probably due to quenching of quasi-free electrons as described above, which does not affect the yield of $Py^{+}\cdot$.

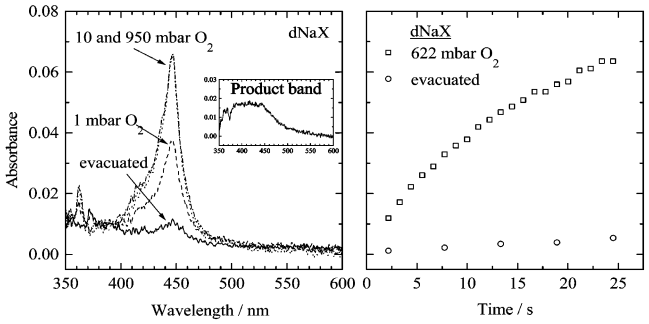

Figure 3. The absorption spectrum produced from lamp irradiation of pyrene in dNaX. The left graph compares the spectrum observed in the evacuated and oxygenated systems. The right graph compares the plot of absorbance *versus* time over the course of a 25-s irradiation period in the evacuated and oxygenated systems. See text for further details.

Further experiments imply that a direct reaction of O_2 with excited states accounts for the increased $Py^{+}\cdot$ yield observed in dNaX. These experiments involve (1) single-photon excitation (or lamp irradiation) of the sample, (2) comparisons of dehydrated and hydrated samples, and (3) measurements of fluorescence. The results are described in the following.

Single-Photon Excitation. To gauge the effectiveness of generating $Py^{+}\cdot$ by reaction of O_2 with ^1Py or ^3Py, an experiment was carried out whereby the sample was irradiated with a relatively low-intensity light source (i.e., a 450 W xenon lamp). In this experiment the growth of $Py^{+}\cdot$ was monitored by absorption spectroscopy over the course of several seconds and while the sample was being irradiated. With this approach any long-lived or stable $Py^{+}\cdot$ that is produced can be detected. With lamp irradiation of the sample, two-photon ionization of S_1 is not a signficant process because the photon intensity is relatively low and S_1 is short-lived. Two-photon ionization is possible through excitation of long-lived triplet states (T_1), in addition to single-photon ionization through oxidation of either S_1 or T_1 by the zeolite. It is explained (vide infra) that these processes are not significant in the zeolite.

With lamp irradiation of the sample, it was possible to make comparisons based only on a single-photon process and without the convolution of a two-photon process involving S_1. It was determined here that with laser excitation of the sample the $Py^{+}\cdot$ yield could always be lowered by the addition of one bar O_2 to the sample. This was true even at low pulse powers which generated $Py^{+}\cdot$ near the lowest level of detection. In general, it was determined that the two-photon process was difficult to avoid by the use of laser excitation of the sample.

The electronic absorption spectrum of ground-state pyrene in solution exhibits strong bands in the region of 300−350 nm.[34] Published absorption spectra of pyrene in NaX and NaY show a similar result.[35] In response to a reviewer's comment, the ground-state spectrum of pyrene in hydrated and dehydrated forms of both NaX and NaY was measured and added to the Supporting Information. The spectra are highly representative of pyrene such that any impurity effects can be ruled out. These spectra are referred to once again in the Discussion.

Figure 3 (left graph) illustrates the visible absorption spectrum observed following lamp irradiation of pyrene in dNaX. Spectra were collected at various P_{O_2} following a 25-s period of irradiation. Collimated and cutoff-filtered light was used to

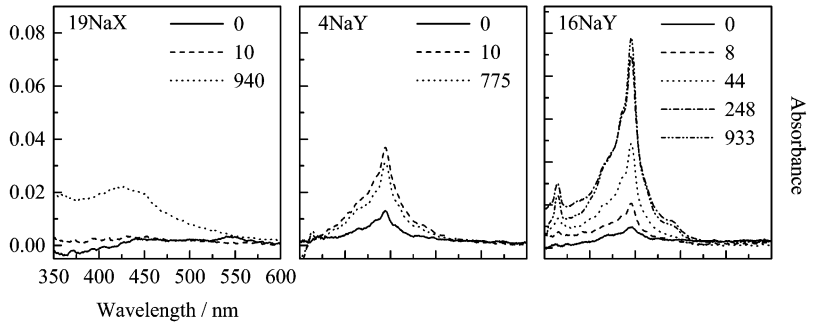

Figure 4. The absorption spectrum produced from lamp irradiation of pyrene for 25 s in samples of hydrated NaX and NaY. The legend refers to values of P_{O_2} in mbar.

excite pyrene in the region $\lambda > 300$ nm. The OD of the sample was monitored in the diffuse transmittance mode by using the Xe lamp as the source of analyzing light (in addition to its use as the source of excitation) and by use of a fiber optic-coupled CCD array spectrometer. The data correspond to the OD spectrum collected with an integration time of 250 ms at the end of the 25-s irradiation period. A background correction was made with an integration time of 250 ms at the start of the irradiation period. At $P_{O_2} = 10$ mbar, the yield of $Py^{+}\cdot$ was significantly higher than in the evacuated sample. A minor peak at 362 nm is observed in Figure 3, but cannot be assigned to $Py^{+}\cdot$. An increase in P_{O_2} to 622 mbar did not alter the $Py^{+}\cdot$ yield, although a significantly lower yield was observed at $P_{O_2} = 1$ mbar. There was a noticeable product band (see inset) with onset at 550 nm following irradiation in the presence of O_2. Longer irradiation times produced more product. The sharp downward peaks at 372 and 350 nm in the product band result from photodegradation which appears as either a drop in fluorescence intensity or a decrease in absorbance of the ground state. The product band was measured by allowing the sample to evolve in the dark for a few minutes following the 25-s irradiation period, followed by a second exposure in which the spectrum was collected in the initial 250 ms of the exposure. This procedure led to minimal $Py^{+}\cdot$ in the product band. The time course of $Py^{+}\cdot$ formation was also followed in dNaX and is also illustrated in Figure 3 (right graph). The $Py^{+}\cdot$ concentration builds more quickly at first and appears to be approaching a steady-state value. In the evacuated system there is little growth of $Py^{+}\cdot$.

The growth of $Py^{+}\cdot$ in oxygenated dNaX was also examined by lamp irradiation at other wavelengths. Irradiation at $\lambda > 375$ nm, or outside of the pyrene absorption spectrum produced no observable $Py^{+}\cdot$ in either the presence or absence of O_2. If photons of $\lambda < 300$ nm were allowed to impinge on the sample (by using quartz optics rather than optical glass), results similar to those in Figure 3 were observed. In other words, excitation with photons of higher energy did not change the results.

One other possible mechanism for generating $Py^{+}\cdot$ is through reaction of ground-state pyrene with singlet oxygen to yield $Py^{+}\cdot$ and superoxide. It is well-established that the reaction of triplet (ground-state) oxygen with triplet pyrene produces singlet oxygen and that the pyrene triplet is produced upon excitation of pyrene in the zeolite. Previous studies have utilized methylene blue (MB) as a sensitizer to produce singlet oxygen for reaction in the zeolite,[17b] and such an approach was used here. The experiment was carried out by loading sequentially 0.005 MB/supercage (from water) and 0.002 pyrene/supercage (from cyclohexane) in dNaX, followed by lamp irradiation of the light blue sample at $\lambda > 375$ nm in the presence of 1 bar O_2. At $\lambda > 375$ nm, only methylene blue is excited and can react with O_2. These conditions generated no $Py^{+}\cdot$ relative to samples not containing methylene blue, indicating that singlet oxygen is not involved.

In evacuated dNaY, lamp irradiation of pyrene at $\lambda > 300$ nm generated a similarly small amount of $Py^{+}\cdot$ compared to dNaX. However, in oxygenated (up to $P_{O_2} = 1$ atm) dNaY, there was no observable increase in the yield of $Py^{+}\cdot$ relative to the evacuated sample. Thus, with respect to the change in $Py^{+}\cdot$ yield at low P_{O_2}, the laser and lamp irradiation experiments produced similar relative results: there was no increase in yield in dNaY and a signficant increase in dNaX when O_2 was added to the sample.

The lamp irradiation experiments provide a potentially useful and unambiguous perspective over the laser experiments on the conditions leading to the generation of $Py^{+}\cdot$ by an O_2-mediated, single-photon process. This process was further assessed as a function of water content in the zeolite.

Influence of H_2O on O_2-Mediated Generation of $Py^{+}\cdot$. O_2-mediated generation of $Py^{+}\cdot$ was examined at various water contents in NaX and NaY. Here the water content is expressed in terms of the number of H_2O per supercage. Because of its small size and polarity, water occupies both the α (supercage) and β (sodalite) cage in zeolites X and Y. On the basis of the void volumes of the α and β cages and the density of water, the maximum number of H_2O that can occupy the α and β cages is ca. 28 and 4, respectively, at room temperature.[1] The hydrated systems are given the abbreviations ϕNaX or ϕNaY, where ϕ represents the number of H_2O present per supercage.

Figure 4 illustrates the OD spectrum following irradiation of pyrene in samples of NaX and NaY at various levels of hydration. In 19NaX (left graph), only a product band was observed at $P_{O_2} = 940$ mbar, while no $Py^{+}\cdot$ or product was observed at $P_{O_2} = 9$ mbar. No identification of the product was attempted. Similar results were observed in 6NaX (data not shown). While the formation of long-lived $Py^{+}\cdot$ was deterred by adding even a small amount of water to NaX, the opposite was observed for NaY. As illustrated in Figure 4 (middle and right graphs), $Py^{+}\cdot$ was generated in either 4NaY or 16NaY, with a more significant effect in 16NaY. The data also indicate a gradual increase in $Py^{+}\cdot$ in 16NaY as P_{O_2} approaches 1 bar. This result is different from that observed in dNaX, where only 10 mbar O_2 produced the maximum yield. The difference can be explained on the basis of a direct electron transfer between S_1 and O_2 to yield $Py^{+}\cdot$ and superoxide ($O_2^{-}\cdot$). In 16NaY, the rate of diffusion-controlled quenching of S_1 by O_2 is lower relative to dNaX, due to blocking effects by water (see Table 1 below in the section on fluorescence studies). Thus, in 16NaY more O_2 is needed to react with S_1 before it decays.

The results thus far imply that $Py^{+}\cdot$ can be produced in the zeolite through a direct, singlet electron transfer to O_2. Although

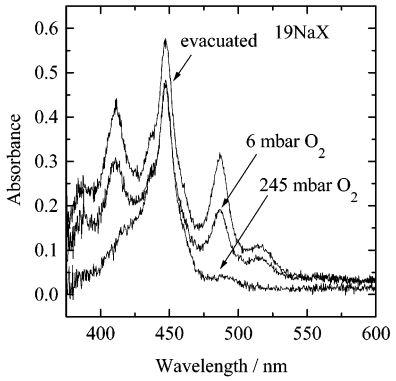

Figure 5. The effect of P_{O_2} on the absorption spectrum measured at 12 μs following 266-nm, 5-ns pulsed laser excitation of pyrene in 19NaX.

no attempts have been made in this study to detect superoxide (we can only speculate its formation due to lack of facility), a previous study has shown by using EPR spectroscopy that superoxide is generated from the UV/O_2 photolysis of naphthalene on dehydrated silica gel and alumina.[36] In the same study, a mechanism involving oxidation by singlet O_2 (or a Type II mechanism) was ruled out. Subsequent studies have shown similar results for the UV/O_2 photolysis of pyrene on silica gel.[37]

With the assumption of superoxide formation in the present systems, a fraction of the superoxide generated in 16NaY must escape the cage in which it was formed such that it does not immediately undergo either cage recombination or reactions with the parent cation, $Py^{+}\cdot$. Laser-based studies provide a useful means of inferring the stability of $Py^{+}\cdot$ in the hydrated systems and assist the interpretation of the results in Figures 3 and 4.

By using pulsed laser excitation, $Py^{+}\cdot$ can be produced in either the presence or absence of O_2 and its reactivity monitored in the time-resolved mode. Figure 5 illustrates the absorption spectrum in 19NaX at 12 μs following pulsed excitation at 266 nm. In evacuated 19NaX, ^{3}Py, $Py^{-}\cdot$, and $Py^{+}\cdot$ are all observed in significant yields, whereas only $Py^{+}\cdot$ is observed at $P_{O_2} =$ 242 mbar. Similar results were observed in 16NaY (data not shown). It should be pointed out that in 16NaY and 19NaX two-photon ionization of pyrene is unaffected at all O_2 pressures up to 1 bar. In these systems the rate of singlet quenching is ca. 10^4 s^{-1} $Torr^{-1}$ (see Table 1 below), which is much lower than in the dehydrated systems. In fully hydrated zeolites, quenching of pyrene fluorescence by O_2 is not observed.

The absence of Na_4^{3+} in Figure 5 can be explained by the more favorable formation of water cluster trapped electrons (e_w^-) over Na_4^{3+}, as observed by Thomas and co-workers.[38] In zeolites X and Y, e_w^- absorbs on the red edge of the visible spectrum with a peak at 760 nm, and decays on a time scale less than 5 μs. That e_w^- was present in 19NaX was confirmed through the observation of microsecond decays ($\tau \approx 2$ μs) of absorbance at 650 nm. Figure 6 (left graph) illustrates the effect of O_2 on the decay profile of e_w^- in 16NaY. Gaussian fits to the decays are included in the graph and are acceptable. The right graph in Figure 6 illustrates a Stern−Volmer plot of the decay rate of e_w^- versus P_{O_2}. The slope yields a rate constant of 9×10^4 s^{-1} $Torr^{-1}$ for the reaction of e_w^- with O_2 to give superoxide. Previous studies which utilized pulsed radiolysis have shown that the rate constant for quenching of e_w^- by O_2 in NaX at water contents higher than used here is 7×10^4 s^{-1} $Torr^{-1}$. The small difference between the two values is probably not significant, but may reflect an increase in O_2 mobility at the lower water content.

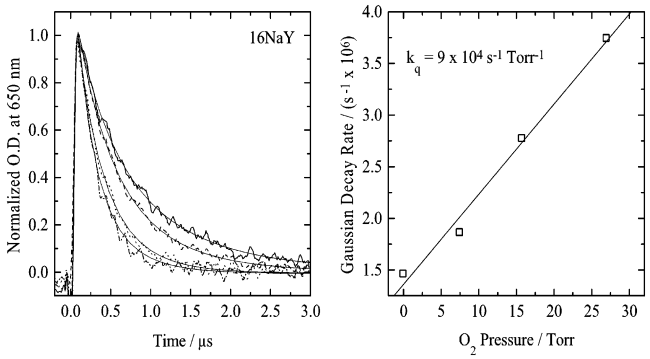

Figure 6. The effect of P_{O_2} on the decay time of water-cluster trapped electrons in 16NaY. The left graph illustrates the decay profiles and the right graph the decay rate as a function of P_{O_2}.

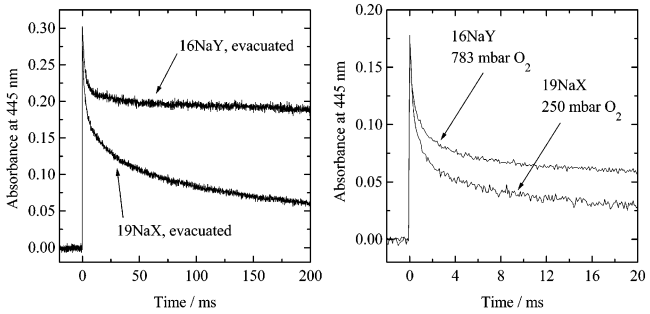

Figure 7. Millisecond decay profiles of absorbance at 445 nm following 266-nm, 5-ns pulsed laser excitation of pyrene in 16NaY and 19NaX. The left and right graphs illustrate the decay profiles in evacuated and oxygenated systems, respectively.

The normalized decay profiles of absorbance at 445 nm in evacuated 19NaX and 16NaY over the course of 200 ms are illustrated in Figure 7 (left graph). A comparison of the two profiles indicates that $Py^{+}\cdot$ is less stable in 19NaX. In 16NaY, the rapid decay component observed in the initial 25 ms is from the decay of overlapping ^{3}Py and $Py^{-}\cdot$ bands, and accounts for about 25% of the absorbance at $t = 0$ (see below). These overlapping components are not as vivid in 19NaX because of the more rapid decay of $Py^{+}\cdot$. The right graph in Figure 7 illustrates the normalized decay profiles of $Py^{+}\cdot$ in oxygenated 16NaY and 19NaX over a time interval of 20 ms. At $P_{O_2} > 5$ mbar, ^{3}Py and $Py^{-}\cdot$ are both quenched on a time scale < 100 μs and only $Py^{+}\cdot$ is observable on a millisecond time scale in the presence of these or higher amounts of O_2. It is clear that the addition of O_2 accelerates the decay of a fraction of $Py^{+}\cdot$. This result is most likely due to a reaction of $Py^{+}\cdot$ with superoxide that is produced through the reaction of O_2 with either e_w^- or excited states. The effect is more pronounced in 19NaX, leading to the complete decay of $Py^{+}\cdot$ within 150 ms (data not shown). A similar effect was observed in 6NaX. In 16NaY, a fraction of the $Py^{+}\cdot$ is unreactive or stable to several seconds.

In 16NaY, the stability of $Py^{+}\cdot$ was dependent on P_{O_2}. Figure 8 shows that as P_{O_2} increases, the yield of long-lived $Py^{+}\cdot$ decreases. A similar effect was observed in 19NaX (data not shown). These results can be interpreted on the basis of the involvement of superoxide as follows. At low P_{O_2} (e.g., 10 mbar), a fraction of e_w^- and excited states escape reaction with O_2 and only a small amount of superoxide is formed. However, as P_{O_2} increases, more superoxide is formed. Using the rate constant determined above for quenching of e_w^- in 16NaY, the rate of quenching of e_w^- is 6.8×10^5 s^{-1} and 6.8×10^7 s^{-1} at $P_{O_2} =$ 10 mbar and 1000 mbar, respectively. These rates can

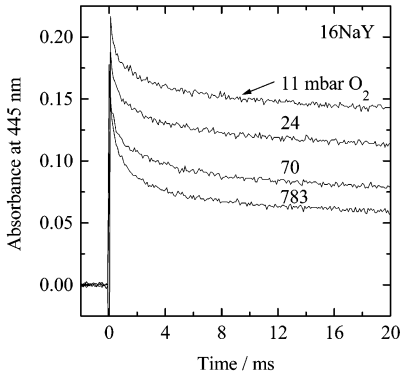

Figure 8. Variation with P_{O_2} in the millisecond decay profiles of absorbance at 445 nm following 266-nm, 5-ns pulsed laser excitation of pyrene in 16NaY.

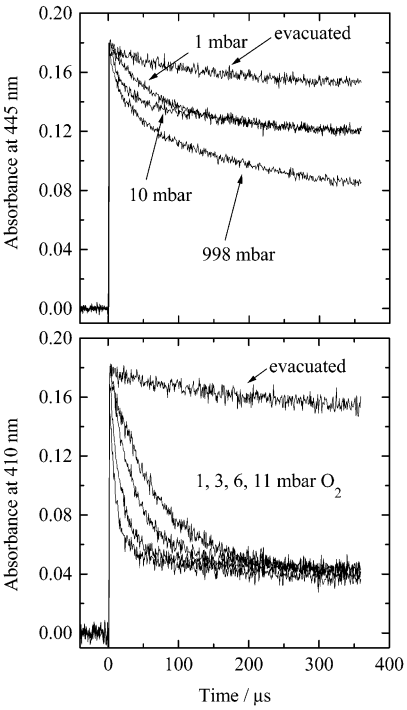

Figure 9. Variation with P_{O_2} in the microsecond decay profiles of absorbance at 445 nm (upper graph) and 410 nm (lower graph) following 266-nm, 5-ns pulsed laser excitation of pyrene in 16NaY. The lower graph illustrates the decay profiles of triplet pyrene.

be compared to the observed decay rate of e_w^- in evacuated 16NaY, which is 1.5×10^6 s^{-1}. Thus, as P_{O_2} increases, there is greater probability for reaction of O_2 with e_w^- and more superoxide is produced. On the other hand, two-photon generation of $Py^{+}\cdot$ is not affected by P_{O_2} in 16NaY. Thus, regardless of P_{O_2} in 16NaY, the intial yield of two-photon generated $Py^{+}\cdot$ is the same for an equivalent excitation energy. Evidently, any single-photon generation of $Py^{+}\cdot$ through reaction of excited states with O_2 is small in comparison to that generated by the two-photon process. Otherwise, an increase in yield with P_{O_2}, as occurred in Figure 4, would be observed in Figure 8. That this was not observed indicates that most of the cation seen in Figure 8 originates from a two-photon process. This argument is supported by the data in Figure 9 which is described below. Thus, most of the superoxide produced from laser excitation originates from the reaction of O_2 with e_w^- that is generated by two-photon excitation. As O_2 increases, more superoxide is produced and the yield of the long-lived, two-photon $Py^{+}\cdot$ decreases.

The initial intensities in the decay profiles of Figure 8 do not accurately represent the yield of $Py^{+}\cdot$. There were rapid (microsecond) decay processes that cannot be followed by the detector operating in the millisecond mode. An analysis in the microsecond mode clarifies this point.

Figure 9 (upper graph) illustrates the microsecond decay profile at 445 nm in 16NaY and compares evacuated and oxygenated systems. In the evacuated system, the decay is relatively flat. However, at $P_{O_2} = 1$ mbar and 10 mbar, there is a noticeable decay occurring over the course of 200 μs and 50 μs, respectively. A comparison of the decay profiles of the triplet band at these values of P_{O_2} (lower graph) shows that the decay at 445 nm is similar in rate to that of the triplet and thus originates from overlap of the triplet band. At $P_{O_2} = 998$ mbar, the triplet is highly quenched and not observable on the microsecond time scale. Under these conditions, the decay at 445 nm is due entirely to that of $Py^{+}\cdot$. Clearly, more cation is generated at $P_{O_2} = 998$ mbar relative to the evacuated system if the triplet overlap is accounted for in the assessment of initial intensities. A similar effect was observed in 19NaX. The result at 998 mbar in Figure 9 also indicates that the yield of single-photon $Py^{+}\cdot$ is only 25% that of the two-photon $Py^{+}\cdot$, indicating that in fact the two-photon process dominates $Py^{+}\cdot$ generation in the laser studies.

Another important point that should be emphasized is that no decay process corresponding to the decay of e_w^- was observed in the decay profile of $Py^{+}\cdot$ in evacuated 16NaY (see Figure 9). This implies that microsecond recombination of $Py^{+}\cdot$ with e_w^- is not a significant process. Any recombination that occurs must therefore take place on a nanosecond or faster time scale, which is more rapid than the time scale for quenching of e_w^- by O_2. Thus, a recombinative mechanism for the production of $Py^{+}\cdot$ can be ruled out in the hydrated systems as well.

It is useful to compare the data in 19NaX and 16NaY with similar data in the dehydrated zeolites. A comparison of Figure 1 and Figure 7 shows that $Py^{+}\cdot$ is more stable in oxygenated dNaX relative to oxygenated 19NaX. A similar effect was observed in dNaY. If superoxide is formed in both the hydrated and dehydrated systems, then the reaction of pyrene cations with superoxide is apparently not as signficant in the dehydrated systems. There is reason to believe that superoxide is generated and reacting with $Py^{+}\cdot$ in the dehydrated zeolites. Previous EPR studies by Kasai have detected superoxide produced from quenching of trapped electrons by O_2 in NaY.[39] In the present study, the decay of $Py^{+}\cdot$ in dNaX over the course of several seconds (measured through observations of the spectrum at various delay times following the laser pulse) was shorter in the presence of O_2. Also, the decay time of $Py^{+}\cdot$ in the presence of O_2 was significantly shorter in dNaX than in dNaY. The slow rate of reaction in the dehydrated systems could be the result of either slow superoxide diffusion or an activation barrier to the reaction between $Py^{+}\cdot$and superoxide.

The above results illustrate the various conditions under which O_2 affects the yield of $Py^{+}\cdot$ in NaX and NaY. Fluorescence studies provide additional information concerning the effects of P_{O_2} and the origin of differences between NaX and NaY.

Pyrene Fluorescence. Previous studies have illustrated the effects of water on the fluorescence of pyrene included in zeolites X and Y. Essentially, the addition of water leads to an increase in the pyrene monomer fluorescence lifetime and to a more resolved fluorescence spectrum. These effects have been explained by the shielding effect that water has on the interaction of pyrene with site II cations.[40,41] In the present study, the effect

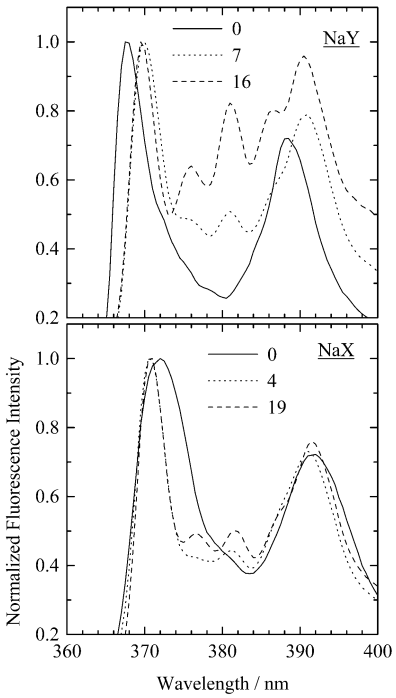

Figure 10. Variation in the pyrene fluorescence spectrum (expanded view) with water content in NaX and NaY. The legend refers to the number of water molecules added per supercage.

of P_{O_2} and small amounts of added water on the pyrene monomer fluorescence spectrum and decay rate was evaluated.

The influence of water on the fluorescence spectrum of pyrene in NaY and NaX is illustrated in Figure 10. A 2-nm hypsochromic shift was observed with the addition of very small amounts of water (i.e., $N_w = 7$) to dNaY. The spectrum at water contents lower than $N_w = 7$ was also examined in NaY, to $N_w = 2$. These spectra were not dramatically different from that in 7NaY and for this reason were not included in Figure 10. It is noteworthy that even in 2NaY the spectrum was noticeably different from that in the dNaY. In 16NaY, the pyrene III/I (or the ratio of the third vibronic band intensity at 381 nm to that of the first or 0−0 transition at 370 nm) was 0.83 and markedly higher than the III/I of 0.55 in 7NaY and 0.25 in dNaY. On the basis of the relationship between pyrene III/I and solvent polarity or dielectric constant,[42] these results imply that the addition of H_2O to NaY significantly lowers the polarity of the pyrene microenvironment. In NaX (lower graph in Figure 10), the addition of water led to a bathochromic shift and to increased resolution. Unlike the results in NaY, no dramatic change in pyrene III/I was observed in NaX.

A fluorescence lifetime analysis revealed a steady increase in average lifetime with added water. The results are illustrated in Figure 11. The dramatic increase in lifetime in both NaX and NaY indicates the shielding effect that water has on the interaction of pyrene with zeolite cations. In dNaY both the lifetime and III/I are much smaller than in dNaX, indicating a more specific interaction of pyrene with dNaY.

The rate constant for quenching of pyrene fluorescence by O_2 was also evaluated in NaX and NaY. Figure 12 illustrates the fluorescence spectrum in NaY at two water contents and at different values of P_{O_2}. Included for comparison is the spectrum in NaX under evacuated conditions. It should be emphasized that the observed changes in fluorescence intensity with P_{O_2} were quite similar in NaX and NaY. Thus the O_2 data for NaX was not included. In the dehydrated zeolites, the majority of the S_1 quanta can be eliminated with only small amounts of

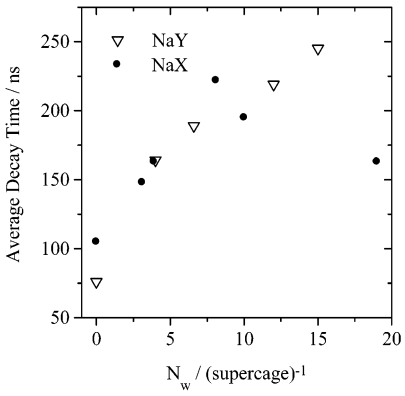

Figure 11. Variation in the lifetime of pyrene fluorescence with water content in NaY and NaX.

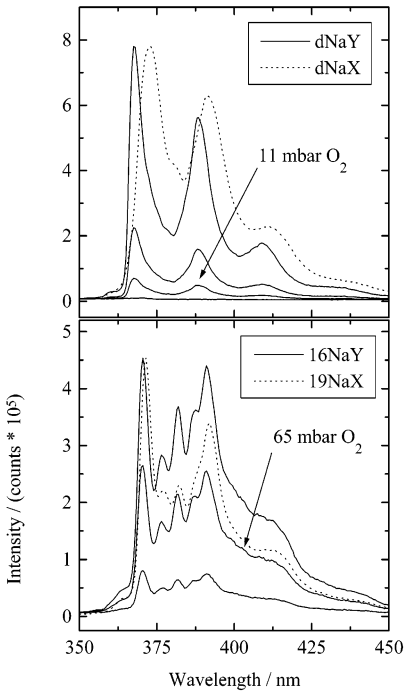

Figure 12. Variation of the pyrene fluorescence spectrum with P_{O_2} in dNaY and 16NaY. Upper graph for dNaY at 375 nm from top to bottom: evacuated, $P_{O_2} = 1$, 11, 950 mbar. Lower graph for 16NaY at 375 nm: evacuated, $P_{O_2} = 65$, 550 mbar. The dashed line in the upper and lower graph illustrates the spectrum in evacuated dNaX and evacuated 19NaX, respectively. The pyrene loading was 0.001/supercage.

added O_2. Even at 1 mbar, about 75% of the quanta have been removed. This was not the case in the hydrated system, where much higher P_{O_2} was required for quenching. This can be explained by the blocking effect that water has on O_2 diffusion.

Figure 13 illustrates the Gaussian-fitted decay profiles of pyrene fluorescence in dNaY and their dependence on O_2 pressure. The fits are quite good; the quenching rate constant (k_q) was determined via a Stern−Volmer analysis from the slope of a plot of $1/\tau$ versus P_{O_2}. A similar approach was used to evaluate k_q at other water contents and in NaX. Table 1 summarizes the results. The values in the dehydrated zeolites are in good agreement with the rates previously reported.[33] It is apparent that small amounts of water $N_w < 6$ do not alter k_q by much. Higher amounts lead to blocking effects. It is important to note that for all the water contents and range of P_{O_2} evaluated, no static quenching of the pyrene fluorescence was observed. This is exemplified by the data in Figure 13, which indicate that the initial intensities (see the values in parentheses) from

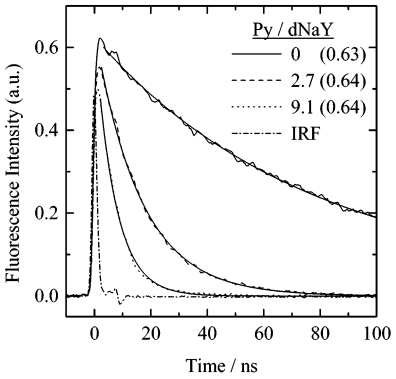

Figure 13. Variation in the decay profiles of pyrene fluorescence with P_{O_2} in dNaY. The solid line illustrates the Gaussian fit to the data. In the legend, the values in parentheses refer to the initial intensity predicted from the Gaussian fit. The values not in parentheses refer to the value of P_{O_2} in mbar. IRF = instrument response function.

TABLE 1: Rate Constants for Quenching of Pyrene Fluorescence by O_2 in NaX and NaY.

zeolite	N_w	k_q (s^{-1} $Torr^{-1}$)	pressure range (Torr)
NaY	0	1.4×10^7	0−9
	4	1.1×10^7	0−9
	16	2.7×10^4	0−760
NaX	0	1.3×10^7	0−9
	6	0.9×10^7	0−9
	19	3.0×10^4	0−760

the Gaussian fits to the data are the same regardless of P_{O_2}. Thus, the quenching is purely dynamic and no evidence for complex formation of O_2 with ground-state pyrene was observed.

Discussion

The results of this study illustrate the influence of O_2 on the yield of photogenerated $Py^{+\cdot}$ in NaX and NaY. Variations in yield were observed, depending on the type of zeolite (NaX or NaY), the degree of hydration of the zeolite, oxygen pressure, and the mode of excitation. For lamp-irradiated samples, an approximate 10-fold increase in the yield of $Py^{+\cdot}$ was observed in dNaX when 0.01−1 bar O_2 was added to the sample. Conversely, in dNaY no increase was observed at any P_{O_2} up to 1 bar. For laser-irradiated samples, similar relative results were observed (i.e., an increase in yield of $Py^{+\cdot}$ in dNaX and no increase in dNaY) when evacuated systems were compared to systems at low P_{O_2}. A comparison at low P_{O_2} was necessary to circumvent the effect that high P_{O_2} has on two-photon ionization of pyrene through S_1. In the hydrated zeolites, lamp irradiation in the presence of O_2 increased the yield of long-lived $Py^{+\cdot}$ in NaY, but not in NaX. The laser studies showed that O_2 increases the yield of $Py^{+\cdot}$ in both 16NaY and 19NaX, but that $Py^{+\cdot}$ was unstable in 19NaX, presumably due to a more efficient reaction of $Py^{+\cdot}$ with water and superoxide. The latter result provides an explanation for why $Py^{+\cdot}$ was not observed upon lamp irradiation of pyrene in oxygenated 6NaX and 19NaX. In 16NaY, a fraction of the laser-generated $Py^{+\cdot}$ was stable for several seconds in the zeolite, regardless of the presence of O_2.

Based upon the above results, it is important to construct a mechanism by which O_2 increases the yield of $Py^{+\cdot}$ in NaX and NaY. For the lamp studies, a two-photon process can be ruled out because the photon intensity is too low and both the singlet and triplet are short-lived in the presence of O_2. On the basis of statistical considerations the rate of triplet quenching should be one-ninth that of singlet quenching,[43] making the triplet lifetime about 1 ns at $P_{O_2} = 1$ bar in dNaX and 44 ns at $P_{O_2} = 1$ bar in 19NaX. These decay times are shorter than those of S_1 in the evacuated systems where the cation yield was low, and therefore cannot support a mechanism involving excitation of T_1.

A single-photon mechanism could involve two processes. One is the reaction of O_2 with either S_1 or T_1 to generate $Py^{+\cdot}$ and superoxide. This reaction may not be an elementary step and could involve singlet oxygen. A second process is the reaction of O_2 with photoejected or trapped electrons that would otherwise recombine with $Py^{+\cdot}$. The latter process does not explain the observed difference between dNaX and dNaY. It is well-known that NaY is more electrophilic (or less electronegative) than NaX.[44,45] Therefore, it is expected that dNaY would react with ^1Py to give $Py^{+\cdot}$ and Na_4^{3+} at least as efficiently as dNaX. It was indicated above that Na_4^{3+} reacts with O_2 at essentially the same rate in dNaY and dNaX. Given this result and barring any differences in rates of $Py^{+\cdot}-Na_4^{3+}$ recombination, it is reasonable to expect that $Py^{+\cdot}$ would be produced in dNaY, at least to the same extent as in dNaX, if a recombinative mechansim was operative. That this was not the case reflects either that the direct electron-transfer mechanism is operative or that the rates of recombination are different.

It should be emphasized that in the *evacuated* systems, the generation of trapped electrons is much less efficient for single-photon ionization relative to two-photon ionization. Two-photon ionization places excess photon energy as kinetic energy in the photoejected electron. The excess energy allows the electron to escape the electric field of the parent cation and avoid recombination. In the zeolite, trapped electrons produced in this way must be located in sodalite cages beyond those adjacent to the parent cation, and any recombination that occurs must occur by a diffusive process. The observed stability of laser-generated $Py^{+\cdot}$ in the dehydrated systems reflects the fact that diffusive recombination of $Py^{+\cdot}$ and Na_4^{3+} is not a significant process. That both of these species are essentially immobile in the zeolite was described in previous studies of quenching of pyrene triplets[27] and theoretical[46] and EPR[47] studies of Na_4^{3+} trapped electrons. For single-photon ionization, the majority of the trapped electrons would be produced as a result of a reaction between excited states and the zeolite, and are likely to be located in one of the four sodalite cages adjacent to the supercage of the parent cation. With this arrangement, recombination would be most efficient and highly competitive with the rate of quenching of Na_4^{3+} by O_2. For example, in dNaX at $P_{O_2} = 10$ mbar, the rate of quenching of Na_4^{3+} by O_2 is 3×10^5 s^{-1}. There was no evidence for recombination on a microsecond or slower time scale that would be affected by this rate of quenching.

Early studies by Thomas and co-workers showed that prolonged lamp irradiation of pyrene in dNaX and dNaY generated $Py^{+\cdot}$, albeit with very low (<0.01) quantum yields.[48] The effect was attributed to the action of a small number of acidic adsorption sites that could be neutralized by the addition of ammonia to the sample. In the present study a relatively small amount of $Py^{+\cdot}$ was generated by lamp irradiation of pyrene in evacuated samples of dNaX and dNaY, probably as a result of the acidic sites. These sites generally do not have much effect in the present systems.

Considering the above arguments, a recombinative mechanism can be ruled out. Thus, a reaction of O_2 with either S_1 or T_1 to generate $Py^{+\cdot}$ and superoxide (or a type I process) very likely explains the effect. While no studies have been carried

out here to detect superoxide, we have pointed out that superoxide was detected in previous work on the UV/O_2 photolysis of naphthalene on silica gel.[36] In addition, the reaction of $Py^{+}\cdot$ with superoxide offers a reasonable explanation for the difference in $Py^{+}\cdot$ stability in 19NaX and 16NaY, and why the lifetime of $Py^{+}\cdot$ was generally lower in oxygenated dNaX and dNaY relative to evacuated conditions.

Some questions remain concerning the mechanism of the reaction of O_2 with S_1 or T_1. It has been established both in solution[47] and on silica surfaces[48] that O_2 enhances S_1-T_1 intersystem crossing in aromatics. Such a mechansim increases the yield of T_1 and involves as an initial step the reaction of O_2 with S_1. It is therefore dependent on all of the factors which control quenching of S_1 by O_2. The triplets so-produced may react directly with O_2 to give $Py^{+}\cdot$ and superoxide, or they could react to give singlet oxygen and ground-state pyrene. For the latter case, singlet oxygen could react with ground-state pyrene to give $Py^{+}\cdot$ and superoxide (a type II process). The propensity for reaction with singlet oxygen can be tested by adding as a sensitizer methylene blue, which upon excitation in the presence of O_2 yields singlet oxygen. While singlet oxygen may be reactive with the zeolite itself, there are examples of MB-sensitized singlet oxygen reactions in zeolites.[17] In the present study, lamp irradiation of MB in oxygenated and pyrene-impregnated dNaX did not generate $Py^{+}\cdot$. Thus, a type I process is favored.

The type I mechanism must be able to explain the difference between dNaX and dNaY. In order for $Py^{+}\cdot$ to be produced, the excited state must yield an electron to O_2 to form superoxide. Once superoxide is formed, it must diffuse away to escape back-reaction with $Py^{+}\cdot$. A reasonable means of charge separation would involve the absorption of excess excitation energy as translational energy by superoxide. To explain the difference between dNaX and dNaY, the electronegativity principles must be invoked. As alluded to above, NaX is more basic (or more electronegative) than NaY. It is also true that pyrene is strongly adsorbed to these zeolites. For this reason it is possible that the excited state is more nucleophilic in dNaX than in dNaY and thus more likely to give up an electron to O_2. In dNaY, the S_1 lifetime was about one-half that in dNaX and the III/I was much lower. These results indicate a more specific interaction of pyrene with dNaY or that pyrene experiences a more polar medium in dNaY. Considering the unusually low III/I observed in dNaY, it can be stated that the pyrene fluorescence is out of the ordinary in dNaY. This may reflect of a type of charge-transfer interaction[51] that draws electron density out of pyrene and prohibits reaction with O_2. In dNaX, the fluorescence is closer to normal, presumably due the higher basicity of NaX that counters the acidity influence of the cations.

It may be that the pyrene fluorescence is an indicator of the oxygen effect. Indeed, when only a small amount of water was added to dNaY, there was a dramatic increase in the fluorescence lifetime and III/I, and it became possible to generate $Py^{+}\cdot$ in the presence of O_2. This can be explained by the shielding effect that water has on the interaction of pyrene with site II cations. Some additional experiments were carried out whereby pyrene was lamp-irradiated on samples of dehydrated ($T_a = 150$ °C) silica gel (Davisil 60) and silica−alumina. For this study, the experimental conditions (i.e., pyrene loadings, sample geometries, etc.) utilized were similar to those utilized for the zeolites. On the surface of both of these solids, $Py^{+}\cdot$ increased in a fashion similar to that in dNaX when O_2 was added to the sample. On these surfaces, the pyrene fluorescence exhibited no unusal characteristics in terms of spectral resolution and lifetime relative to that observed in typical polar organic solvents, such as methanol.[42] The fluorescence of pyrene in dNaY is quite unusual compared to what is typically observed for pyrene.

One reviewer suggested that dNaX may have contained significant amounts of moisture. However, the thermal treatment used to dehydrate the samples (i.e., evacuation of pyrene-loaded samples at 125 °C for 15 min) was shown in ref 27 to produce the same water content as heating the sample for several hours in air at 550 °C. While heating in air at 550 °C may not completely dehydrate the sample, this author believes the water contents are low enough to be comparable to the completely dehydrated zeolites. One has to take into account the dramatic changes that have been observed in this study upon the addition of only small amounts of water to dNaX and dNaY.

While high acidity may explain why $Py^{+}\cdot$ was not generated in dNaY, it could be argued that dNaY is *less* polar than dNaX, and that the lower polarity in dNaY inhibits charge separation. Previous studies have attempted to measure polarity or dielectric constant in the zeolites X and Y on the basis of the positions of ground-state absorption bands of various probe molecules.[20] In the present study, the pyrene absorption band in dNaY is blue-shifted by 3 and 4 nm relative to that in dNaX and 16NaY, respectively (see Supporting Information). Similar effects are observed when the fluorescence bands are compared. These results support the argument that dNaY is less polar than dNaX. However, the assignment of band positions to dielectric constant requires a solvent continuum, which cannot be assumed at the vacuum−solid interface in solvent-free zeolites. To shed light on this topic, some additional experiments were carried out in which cyclohexane was added to dNaY at a level of 2.5 per supercage, or about one-half the maximum loading possible. Such a loading produced a red-shift of 3 nm in the absorption spectrum relative to dNaY, and quenching of S_1 by O_2 at rates similar to that in 16NaY. On the basis of band positions, it could be argued that the polarity of the cyclohexane-loaded dNaY is higher than in dNaY and equivalent to that of dNaX. Nonetheless, lamp irradiation of pyrene in dNaY/cyclohexane containing 1 bar O_2 did not generate $Py^{+}\cdot$ to any extent greater than that observed in oxygenated dNaY where the yield was relatively small. On the other hand, it was possible to generate $Py^{+}\cdot$ in dNaX/cyclohexane containing 1 bar O_2, although the yield was only about one-half that in dNaX. These results point out that there is no correlation between the positions of ground-state absorption bands and the ability of the zeolite to support charge separation.

Further support for the type I mechanism comes from the fluorescence studies. It was shown that in either dNaX or dNaY, low O_2 pressures (i.e., 10 mbar) remove the majority of S_1 quanta. This result explains why in dNaX there was not much difference in the yield of $Py^{+}\cdot$ when the low and high O_2 pressures were compared. Only at $P_{O_2} = 1$ mbar was a lower yield of $Py^{+}\cdot$ observed, and this coincided with the increase in fluorescence quanta observed at $P_{O_2} = 1$ mbar relative to $P_{O_2} = 10$ mbar. In 16NaY, S_1 was not as efficiently quenched due to blocking effects by H_2O and much more than 10 mbar O_2 was needed to maximize the yield of $Py^{+}\cdot$.

Previous studies have introduced a relatively new approach to selective photocatalyzed oxidation of both saturated and unsaturated hydrocarbons.[15,24] In this approach, excitation of an identifiable molecular-O_2 contact charge-transfer (CT) complex is carried out in the supercages of alkali and alkaline-earth metal ion-exchanged zeolites X, Y, and L. In solution, the CT complexes of interest typically absorb in the near UV

region. In dehydrated zeolites the strong electrostatic field imposed on adsorbates by the zeolite cations shifts the absorption of the CT complex from the near UV to the visible region of the spectrum. Excitation in the visible region lowers the energy of the radical intermediates involved and leads to increased product selectivity through control of radical scrambling. Excitation at UV wavelengths may excite the CT complexes in the zeolite, but could also produce excited states and excess energy in the products. It is useful to discuss the possibility that $Py^{+}\cdot$ is produced through excitation of a pyrene$-O_2$ CT complex at UV wavelengths.

At room temperature, the formation of a molecular-O_2 contact CT complex involves a weak equilibrium or low stabilization energy ($< kT$).[52] For this reason, high P_{O_2} (i.e., 0.5−1 bar) is necessary to be able to observe the charge-transfer absorption in zeolites.[15,24] In the present study, there was no observable difference in the yield of $Py^{+}\cdot$ at $P_{O_2} = 10$ mbar and 1 bar in dNaX. If a CT complex was involved, a higher yield would be expected at $P_{O_2} = 1$ bar. A closer relationship exists between fluorescence quenching that occurs with increasing P_{O_2} and the increase in yield of $Py^{+}\cdot$. Thus, the favored path is a reaction of O_2 with the excited state and not through excitation of a CT complex.

The results of the present study are in accord with those of previous studies of the oxygen-induced photochemistry of pyrene on the surface of silica gel.[37] It was proposed that, on silica surfaces, O_2 reacts with excited states to yield $Py^{+}\cdot$ which subsequently reacts with H_2O to give mainly pyrenediones and small amounts of 1-hydroxypyrene. Thus, O_2 promotes the photodegradation of pyrene on the surface and the formation of water-soluble pyrene derivatives. A type II mechanism could not explain the results on silica and a type I mechanism was favored.

Of further interest is the role of O_2 in stimulating cation radical formation by photoexcitation of other types of molecules in zeolites. Ionization potential is likely to have a significant effect, but this has not yet been verified. Ramamurthy and co-workers have shown that short wavelength (<300 nm) excitation of 1,1-diarylethylenes in NaY produced 1,1-diarylethane as the major product when the zeolite was bathed in O_2-saturated hexane.[16] Of significance was that the quantum yield of the diarylethane was much less in the absence of O_2. To explain the effect, a mechanism was proposed whereby O_2 reacts with Na_4^{3+}-trapped electrons that would otherwise recombine with cation radicals. It was also proposed that the trapped electrons and cation radicals were produced as a result of the reaction of excited states with the zeolite, or by a single-photon reaction. Following the formation of the radical cation, hydrogen atom abstraction yields the diarylethane. While the reaction of O_2 with trapped electrons certainly occurs, we have pointed out that this reaction is too slow to be of significance in stopping recombination of pyrene cation radicals, especially when single-photon ionization is involved. Further, for samples bathed in hexane, the O_2 concentration and the rate of O_2 diffusion are much lower than in the dry (unsolvated) zeolite. We are currently investigating these and other types of unclarities involving electron-transfer reactions in zeolites in order to arrive at a more unified understanding of this process.

Conclusion

Previous studies have described the rates of quenching of pyrene luminescence by O_2 in zeolites. While these studies have described the conditional requirements for quenching, they have not shown that cation radicals are generated by the reaction of excited states with O_2. The present study has confirmed that such a reaction occurs and has demonstrated the methodolgy by which the cation radicals can be monitored. The lamp-based methodology provided an unambiguous means by which to produce and monitor long-lived cation radicals of interest, and was complimentary to the laser-based studies. It is important to show the conditions under which stable cation radicals can be produced through the reaction of excited states in zeolites.

This study has pointed out some conditional requirements for the generation of pyrene cation radicals from the electron-transfer reaction of excited states with O_2. In dNaX, cation radicals were produced in accord with observations made in other systems, including the surface of dehydrated silica and silica−alumina. No cation radicals were produced in dNaY. These differences have been explained by an unusual interaction of pyrene with dNaY that lowers the nucleophilicity of the excited state and inhibits charge separation. In hydrated NaY, water weakens the interaction with the zeolite, resulting in behavior that is more in accord with the other systems. These results illustrate that the zeolite medium is not necessarily advantageous for achieving charge separation despite the strongly polarizing influence that zeolite cations have on stabilizing charged intermediates. Interactions of excited states with the zeolite have to be considered. In NaY, the presence of water promotes charge separation. More studies are needed to clarify the relationship between bimolecular electron transfer and the nature of the zeolite.

Acknowledgment. The author thanks the Office of Research and Sponsored Programs and the College of Liberal Arts at the University of Mississippi for support of this work.

Supporting Information Available: Ground-state absorption spectrum of pyrene in zeolites. This material is available free of charge via the Internet at http://pubs.acs.org.

References and Notes

(1) Breck, D. W. *Zeolite Molecular Sieves: Structure, Chemistry, and Use*; John Wiley and Sons: New York, 1974.
(2) Barrer, R. M. *Zeolites and Clay Minerals as Sorbents and Molecular Sieves*; Academic Press: New York, 1978.
(3) Dyer, A. *An Introduction to Zeolite Molecular Sieves*; John Wiley & Sons: New York, 1988.
(4) Flanigen, E. In *Zeolites: Science and Technology*; Ribeiro, F., Rodrigues, A., Rollmann, L., Naccache, C., Eds; Martinus Nijhoff Publishers: Boston, 1984.
(5) Turro, N. J. *Acc. Chem. Res.* **2000**, *33*, 637.
(6) Turro, N. J. In *Molecular Dynamics in Restricted Geometries*; Klafter, J., Drake, J. M., Eds.; John Wiley and Sons: New York, 1989; Chapter 14.
(7) Ramamurthy, V. In *Photochemistry in Organized and Constrained Media*; Ramamurthy, V., Ed.; VCH Publishers: New York, 1991; Chapter 10.
(8) Thomas, J. K. *Chem. Rev.* **1993**, *93*, 301.
(9) Scaiano, J. C.; Garcia, H. *Acc. Chem. Res.* **1999**, *32*, 783.
(10) Cosa, G.; Chretien, M. N.; Galletero, M.; Fornes, V.; Garcia, H.; Scaiano, J. C. *J. Phys. Chem. B* **2002**, *106*, 2460.
(11) Park, Y.; Lee, E.; Chun, Y.; Yoon, Y.; Yoon, K. B. *J. Am. Chem. Soc.* **2002**, *124*, 7123.
(12) Bossmann, S. H.; Turro, C.; Schnabel, C.; Pokhrel, M.; Payawan, L.; Baumeister, B.; Worner, M. *J. Phys. Chem. B* **2001**, *105*, 5374.
(13) Bhuiyan, A.; Kincaid, J. *Inorg. Chem.* **2001**, *40*, 4464.
(14) Vitale, M.; Castagnola, N.; Ortins, N.; Brooke, J.; Vaidyalingam, A.; Dutta, P. *J. Phys. Chem. B* **1999**, *103*, 2408.
(15) (a) Blatter, F.; Sun, H.; Vasenkov, S.; Frei, H. *Catal. Today* **1998**, *41*, 297. (b) Frei, H.; Blatter, F.; Hai, S. *CHEMTECH* **1996**, *26*, 24.
(16) Lakshminarasimhan, P.; Thomas, K.; Hohnston, L.; Ramamurthy, V. *Langmuir* **2000**, *16*, 9360.
(17) (a) Clennan, E. L.; Sram, J. P. *Tetrahedron* **2000**, *56*, 6945. (b) Clennan, E. L.; Sram, J. P. *Tetrahedron Lett.* **1999**, *40*, 5275.
(18) Joy, A.; Warrier, M.; Ramamurthy, V. *Spectrum* **1999**, *12*, 1.
(19) All structural data was taken from ref 1.

(20) Uppili, S.; Thomas, K.; Crompton, E.; Ramamurthy, V. *Langmuir* **2000**, *16*, 265.
(21) (a) Yoon, K. B. *Chem. Rev.* **1993**, *93*, 321. (b) Yoon, K. B.; Hubig, S. M.; Kochi, J. K. *J. Phys. Chem.* **1994**, *98*, 3865. (c) Sankararaman, S.; Yoon, K.; Yabe, T.; Kochi, J. *J. Am. Chem. Soc.* **1991**, *113*, 1419.
(22) Alvaro, M.; Chretien, M. N.; Ferrer, B.; Fornes, V.; Garcia, H.; Scaiano, J. C. *Chem. Commun.* **2001**, *20*, 2106.
(23) Hashimoto, S. *Chem. Phys. Lett*. **1996**, *252*, 236.
(24) (a) Vasenkov, S.; Frei, H. *J. Phys. Chem.* **1997**, *1010*, 44539. (b) Sun, H.; Blatter, F.; Frei, H. *J. Am. Chem. Soc.* **1994**, *116*, 7951. (c) Blatter, F.; Frei, H. *J. Am. Chem. Soc*. **1994**, *116*, 1812. (d) Blatter, F.; Moreau, F.; Frei, H. *J. Phys. Chem.* **1994**, *98*, 13403. (e) Vasenkov, S.; Frei, H. *J. Phys. Chem. B* **1998**, *102*, 8177. (f) Sun, H.; Blatter, F.; Frei, H. *J. Am. Chem. Soc.* **1996**, *118*, 6873.
(25) Takeya, H.; Kuriyama, Y.; Masanobu, K. *Tetrahedron Lett.* **1998**, *39*, 5967.
(26) (a) Larsen, R.; Saladino, A.; Hunt, T.; Mann, J.; Xu, M.; Grassian, V.; Larsen, S. *J. Catal.* **2001**, *204*, 440. (b) Xiang, Y.; Larsen, S. Grassian, V. *J. Am. Chem. Soc.* **1999**, *121*, 5063. (c) Panov, A.; Larsen, R.; Totah, N.; Larsen, S.; Grassian, V. *J. Phys. Chem. B* **2000**, *104*, 5706.
(27) Ellison, E. H. *J. Phys. Chem. B.* **1999**, *103*, 9314.
(28) Albery, J. W.; Barlett, P. N.; Wilde, C. P.; Darwent, J. R. *J. Am. Chem. Soc.* **1985**, *107*, 1854.
(29) (a) Iu, K. K.; Thomas, J. K. *Colloids Surf.* **1992**, *63*, 39. (b) Iu, K. K.; Thomas, J. K. *J. Phys. Chem.* **1991**, *95*, 506.
(30) Koichi, K. *Triplet−triplet absorption spectra*; Bunshin: Tokyo, 1989.
(31) Shida, T. *Electronic absorption spectra of radical ions*; Elsevier: Amsterdam, 1988.
(32) (a) Liu, X.; Iu, K. K.; Thomas, J. K. *J. Phys. Chem*. **1994**, *98*, 13720. (b) Iu, K. K.; Liu, X.; Thomas, J. K. *J. Phys. Chem*. **1993**, *97*, 8165. (c) Liu, X.; Zhang, G.; Thomas, J. K. *J. Phys. Chem*. **1995**, *99*, 10024. (d) Zhang, G.; Liu, X.; Thomas, J. K. *Radiat. Phys. Chem*. **1998**, *51*, 135.
(33) Liu, X.; Iu, K. K.; Thomas, J. K. *J. Phys. Chem.* **1989**, *93*, 4120.
(34) Murov, S. L.; Carmichael, I.; Hug, G. L. *Handbook of Photochemistry*; Marcel Dekker: New York, 1993; p 184.
(35) Liu, X.; Thomas, J. K. *Langmuir* **1993**, *9*, 727.
(36) Barbas, J. T.; Sigman, M. E.; Buchanan, A. C.; Chevis, E. A. *Photochem. Photobiol.* **1993**, *58*, 155.
(37) Reyes, C. A.; Medina, M.; Crespo-Hernandez, C.; Arce, R.; Rosario, O.; Steffenson, D. M.; Ivanov, I. N.; Sigman, M. E.; Dabestani, R. *Environ. Sci. Technol.* **2000**, *34*, 415.
(38) Liu, X.; Zhang, G.; Thomas, J. K. *J. Phys. Chem*. *B* **1997**, *101*, 2182.
(39) Kasai, P. *J. Chem. Phys.* **1965**, *43*, 3322.
(40) Thomas, K. J.; Sunoj, R. B.; Chandrasekhar, J.; Ramamurthy, V. *Langmuir*, **2000**, *16*, 4912.
(41) Hashimoto, S.; Ikuta, S.; Ashai, T.; Masuhara, H. *Langmuir*, **1998**, *14*, 4284.
(42) Kalyanasundaram, K.; Thomas, J. K. *J. Am. Chem. Soc*. **1977**, *99*, 2039.
(43) Birks, J. B. *Photophysics of Aromatic Molecules*; John Wiley and Sons: New York, 1970; p 500.
(44) (a) Barthomeuf, D. *J. Phys. Chem.* **1984**, *88*, 42. (b) Barthomeuf, D. *Catal. Rev. Sci. Eng.* **1996**, *38*, 613.
(45) (a) Sanderson, R. T. In *Chemical Bonds and Bond Energy*; Academic Press: New York, 1976. (b) Sanderson, R. T. *Polar Covalence*; Academic Press: New York, 1983.
(46) (a) Haug, K.; Srdanov, V.; Stucky, G.; Metiu, H. *J. Chem. Phys.* **1992**, *96*, 3495. (b) Blake, N. P.; Srdanov, V.; Stucky, G.; Metiu, H. *J. Phys. Chem.* **1995**, *99*, 2127.
(47) Edwards, P. P.; Anderson, P. A.; Thomas, J. M. *Acc. Chem. Res.* **1996**, *29*, 23.
(48) Liu, X.; Iu, K. K.; Thomas, J. K. *J. Phys. Chem*. **1994**, *98*, 7877.
(49) (a) Turro, N. J.; Renner, C. A.; Waddell, W. H.; Katz, T. J. *J. Am. Chem. Soc.* **1976**, *98*, 4321. (b) Thomas, J. K.; Richards, J. T.; West, G. *J. Phys. Chem.* **1970**, *74*, 4137.
(50) Ruetten, S. A.; Thomas, J. K. *J. Phys. Chem. B* **1999**, *103*, 1278.
(51) Thomas, J. K. Personal communication.
(52) Davidson, R. S. In *Molecular Association*, Vol. 1; Foster, R., Ed.; Academic Press: New York, 1975; p 238.